Perovskite Solar Cells with Near 100% Internal Quantum Efficiency Based on Large Single Crystalline Grains and Vertical Bulk Heterojunctions

Bin Yang,[†] Ondrej Dyck,[‡] Jonathan Poplawsky,[†] Jong Keum,[†] Alexander Puretzky,[†]

Sanjib Das,[§] Ilia Ivanov,[†] Christopher Rouleau,[†] Gerd Duscher,[‡] David Geohegan,[†] Kai Xiao[†]*

† Center for Nanophase Materials Sciences, Oak Ridge National Laboratory, Oak Ridge, TN, 37831, USA.

‡ Department of Materials Science and Engineering, University of Tennessee, Knoxville, TN, 37996, USA.

§ Department of Electrical Engineering and Computer Science, University of Tennessee, Knoxville, TN, 37996, USA.

EXPERIMENTAL SECTION

Materials preparation

The TiO_2 precursor solution was prepared following the method reported by Snaith et al.1a 369 μL titanium isopropoxide (Sigma-Aldrich, used as received) solution and 70 μL 1M hydrogen chloride (HCl) solution (used as received) were separately diluted in 2.53 ml 2-propanol. Subsequently, the diluted HCl solution was added drop by drop into the diluted titanium isopropoxide solution under heavy magnetic stirring. After further stirring for 10 hours, the mixed solution was filtered with a 0.2 mm pore size PTFE filter. The obtained TiO_2 precursor solution was stored in a desiccator for long-term use. The PbI_2 (Sigma Aldrich, used as received) was dissolved in N,N-Dimethylformamide (DMF) with a concentration of 550 mg/mL under heavy magnetic stirring and heating at 100 ^{o}C on a hotplate for 20-30 minutes. The methylammonium iodide (CH_3NH_3I) powder (purchased from 1-Materials, used as received) was dissolved in 2-propanol to make a solution with concentration of 70 mg/mL, which was heated at 100 ^{o}C on a hotplate. The Spiro-OMeTAD powder (purchased from 1-Materials, used as received) was dissolved in chlorobenzene (CB) for a 90 mg/mL solution, and the combination of p-type dopants 10 μL 4-tert-butylpyridine (tBP) and 45 μL lithium bis(trifluoromethane sulfonyl) imide (Li-TFSI) with a concentration of 170 mg/mL (dissolved in anhydrous acetonitrile) was applied to dope the Spiro-OMeTAD. Both tBP and Li-TFSI were purchased from Sigma Aldrich, and used as received. The Spiro-OMeTAD/doping mixture solution was stirred with a magnetic stir bar at 50 ^{o}C overnight.

Device fabrication and characterization

The cleaned ITO glass substrates were treated with UV-Ozone for 10 minutes before the spin coating of as-made TiO_2 precursor solution at 2000 rpm for 60 seconds in air. Subsequently, the TiO_2 precursor substrates were fired in a furnace at 500 ^{o}C for 30 minutes. After the substrates cooled down to room temperature, a 100 ^{o}C PbI_2 solution (550 mg/mL) was spin-coated onto the TiO_2 at 6000 rpm for 30 seconds in an N_2-filled glovebox. The obtained PbI_2 films were then thermally-annealed at 100 ^{o}C on a hotplate for 60 seconds. After the PbI_2 films cooled down, the CH_3NH_3I solution (70 mg/mL) was dropped onto the PbI_2 films and quickly spin-coated at a high-speed of 6000 rpm for 30 seconds to obtain uniform PbI_2/CH_3NH_3I bilayer films. The as-grown bilayer films were then placed in ambient air (humidity of ~30%) for 60 minutes until the color of the films was dark brown. Subsequently, the films were thermally annealed at 100 ^{o}C for 2 hours covered by a glass petri dish in an N_2-filled glovebox. The as-prepared Spiro-OMeTAD solution was dropped onto the obtained perovskite films. After waiting for 5 seconds, they were spin coated at 2000 rpm for 40 seconds, and then left in a desiccator overnight. A top metal contact silver layer with a thickness of 100 nm was deposited using the thermal evaporation method under a vacuum level of 10^{-6} mbar with a deposition rate of 1 Å/s.

The *J-V* curves of the devices were measured in an N_2-filled glovebox with a Keithley 2400 source meter under illumination of 100 mW/cm^2 (AM 1.5 G solar spectrum), which was provided by a solar simulator (Radiant Source Technology, 300 W, Class A). After stabilization, the lamp light intensity was calibrated with Si-reference cell certified by NIST. The *J-V* curves were measured by sweeping from reverse bias (-0.2 V) to forward bias (1.2 V), and forward bias (1.2 V) to reverse bias (-0.2 V), with a 35 mV step size, and 50 ms sweep delay time. During *J-V* curve measurement, we soaked the devices under one-sun illumination for ~ 60 seconds at around maximum power output point before each measurement. We used two different device areas (~6.5 mm^2 and ~23.7 mm^2), which yielded similar J_{SC}. The device areas were carefully measured and calculated using optical microscopy.

For incident photon-to-current efficiency (IPCE) measurement, a power source (Newport, 300 W Xenon lamp) with Oriel Cornerstone monochromator (model 130, 1/8m) was used to illuminate the device. The illumination light source was chopped at 8 Hz and the electrical signal was collected by a lock-in amplifier (Merlin Radiometric Lock-In Amplifier, Newport) under short-circuit conditions. A calibrated silicon diode (70356-70316NS, Newport) with a known spectral response spectra was used as a reference. For the reflective absorption spectrum, the incident light from the ITO electrode side was reflected back into the active layer by the metal electrode for the secondary absorption as shown in the inset of Figure 2d. The reflective absorption spectrum was obtained by measuring in diffuse mode with an integration sphere attachment and referenced against standard Spectra on sample.

X-ray diffraction and X-ray pole figure

The x-ray diffraction (XRD) patterns (θ/2θ scans) were collected using an X-ray diffractometer (Panalytical X'Pert MPD Pro) with Cu-Kα radiation (λ=1.54050Å). The step size and scan rate of for each measurement was 0.0167113^o and 0.107815 ^{o}/s, respectively. The pole figure was measured using an X-ray diffractometer (Panalytical X'Pert MRD Pro) with Cu-Kα radiation (λ=1.54050Å) to find the orientation of the (110) crystal plane of the $CH_3NH_3PbI_3$ with 2θ=14.05^o.

Electron microscopy/electron energy loss spectroscopy

The surface morphological images were taken with a scanning electron microscope (SEM; Zeiss Merlin SEM). The SEM images were acquired by the Inlens model, line average scanning with a gun voltage of 5 kV. The transmission electron microscope (TEM) used in these studies was a Zeiss Libra 200MC operated at 200 kV. The electron energy loss spectroscopy (EELS) images were acquired with a beam current of 158 pA, as measured on the calibrated spectrometer CCD in vacuum, with an exposure time of 0.1 seconds per pixel and a pixel size of 5.3x5.3 nm^2. Spectra were background subtracted and fit with a hydrogenic model scattering cross-section. With a known beam current and calibrated spectrometer, the fitting parameter could be interpreted as atomic areal density, and a quantitative value is obtained within ~10%. Selected area diffraction was taken with an illuminated area of 325 nm for Pattern 1-3 and an illuminated area of 180 nm for Pattern 4-6 as shown in Figure 3a. In order to reduce the beam intensity such that a beam stop was not needed, the monochromator slit was moved to the tail of the beam profile to decrease the beam current (~15 pA) and an exposure time of 0.1 seconds was used. All imaging was acquired under parallel illumination in TEM mode, with the exception of Figure 4d which is a high angle annular dark field (HAADF) image taken in STEM mode. The tested ultra-thin cross-sectional specimens (~50 nm) were prepared by focused ion beam (FIB) milling with a final polish at an accelerating voltage of 10 kV and beam current of 20 pA to minimize beam induced surface damage.

Electron beam induced current mapping

The electron beam induced current/scanning electron microscopy (EBIC/SEM) measurements were done in a Hitachi 4800-CFEG equipped with a Gatan EBIC system. The EBIC currents were amplified by a Stanford Research Systems model SR570 low-noise current preamplifier. An accelerating voltage of 1.5 kV with beam currents of 30–50 pA were used to ensure a high resolution probe with a good signal to noise ratio while maintaining low-injection EBIC conditions. Sample preparation damage can cause surface recombination, which can limit the EBIC measurements. Therefore, cross-sections were prepared by both cleaving and argon ion milling with a Gatan Illion+. Sample cleaving was used for the EBIC results presented in Figure 4a in the main text. The argon ion milled section suffered from damage induced by the argon ion beam and the measured beam currents were very weak. However, the cross-section of this sample is very smooth and also shows high EBIC currents at the grain boundaries (GBs). Therefore, the heavily enhanced EBIC currents at the GBs for the cleaved sample are not completely due to surface topography, and can be explained by a local electric field between the grains and GBs. The measured device cross-sections for each sample preparation method were exposed to air for several minutes prior to loading in the SEM because the samples had to be manually mounted on the EBIC stage. Because of this, each sample was exposed to air for slightly different times depending on the time it took to properly contact the sample. This variation could cause slight changes in the measured EBIC efficiency (proportional to the EBIC current/probe current) between the measured samples regardless of the measured device efficiency. The contrast between the grain boundaries (GBs) and grains (larger GB EBIC with respect to the grain) remained consistent. These samples were very sensitive to electron beam exposure, only allowing for each cross-section area to be scanned one time. After each initial EBIC scan, the measured EBIC degraded regardless of the sample. Overall, a lot of factors could vary the measured EBIC current magnitude.

We should note that our EBIC measurements were done at a very low accelerating voltage (1.5 kV), which means that most of the carrier generation occurs less than 15 nm away from the polish cross-sectional surface. Therefore, the carriers are exposed to surface recombination from the polished surface. This makes the EBIC measurements very sensitive to internal electric fields of the material. Basically, the currents are enhanced in space-charge regions. Under normal operation, current will be collected in the grain interiors much more efficiently than the cross-section EBIC measurements because the exposed cross-sectional surface does not exist, negating the surface recombination.

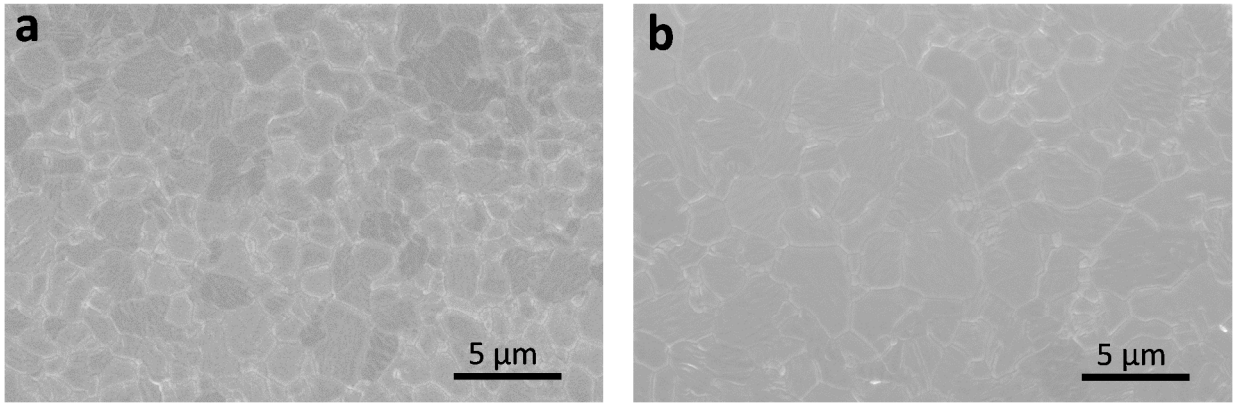

Figure S1. Air-exposure effect on $CH_3NH_3PbI_3$ crystalline grain size: (a) Without air-exposure, the CH_3NH_3I/PbI_2 bilayer films were directly thermal-annealed for 2 hours in a water-free and N_2-filled glovebox; (b) Air-exposure for 1 hour in an ambient environment (humidity of ~30%) at room temperature, and thermally-annealed for 2 hours at 100^{0}C in a water-free, N_2-filled glovebox.

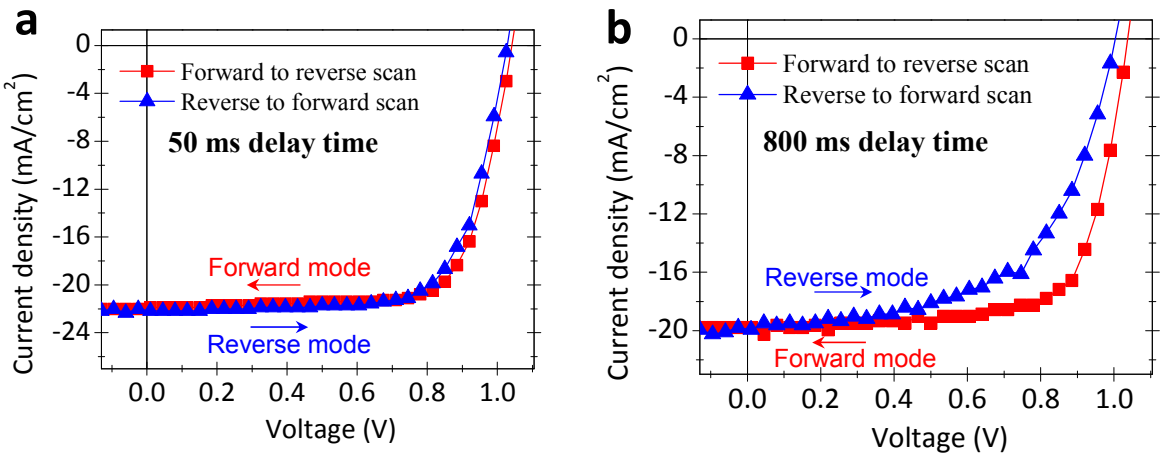

Figure S2. J-V curves obtained from our device measured using sweep delay time 50 ms (a) and delay time 800 ms (b), with forward scan (from forward bias to reverse bias, red curve) and reverse scan (from reverse bias to forward bias, blue curve).

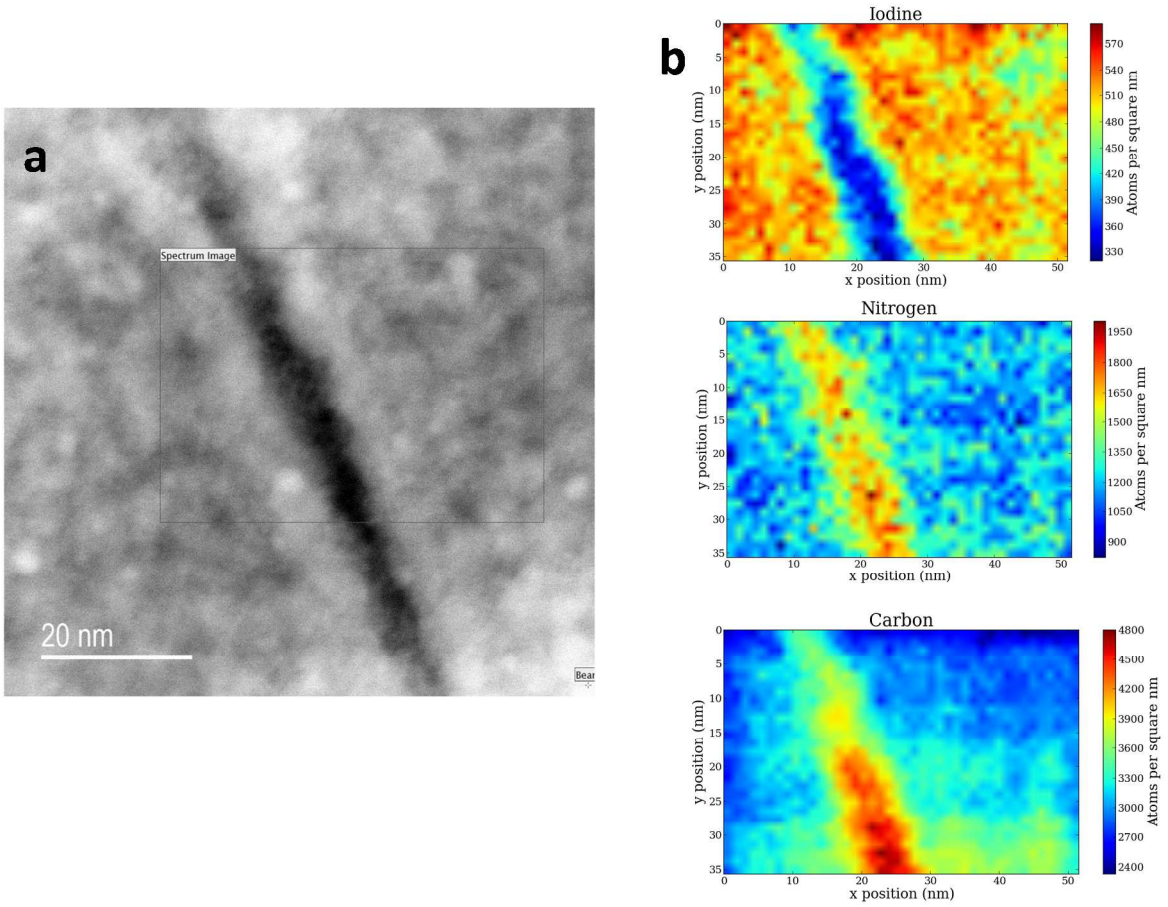

Figure S3. A Zoomed-in STEM image and EELS maps in vicinity of a GB to show the presence of Spiro-OMeTAD in a GB. (a) A zoomed-in Z-contrast dark-field STEM image. (b) Corresponding zoomed-in EELS maps to show both carbon and nitrogen are present, and iodine is absent in GBs.